IEEE Access
Multidisciplinary | Rapid Review | Open Access Journal

Received August 4, 2019, accepted August 16, 2019, date of publication August 21, 2019, date of current version September 6, 2019.

Digital Object Identifier 10.1109/ACCESS.2019.2936553

A Novel Design Method for High Isolated Microstrip Diplexers Without Extra Matching Circuit

XUEHUI GUAN[1], (Member, IEEE), WANG LIU[1], BAOPING REN[1], (Student Member, IEEE), HAIWEN LIU[2], (Senior Member, IEEE), AND PIN WEN[2], (Student Member, IEEE)

[1]School of Information Engineering, East China Jiaotong University, Nanchang 330013, China
[2]School of Electronics and Information Engineering, Xi'an Jiaotong University, Xi'an 710049, China

Corresponding author: Baoping Ren (baoping1988@hotmail.com)

This work was supported in part by the National Science Foundation Committee of China under Grant 61761018, Grant 61461020, and Grant 61901170, in part by the Jiangxi Provincial Cultivation Program for Academic and Technical Leaders of Major Subjects, China, under Grant 20162BCB22018, in part by the Natural Science Foundation of Jiangxi Province, China, under Grant 20181BBE58016, Grant 20171BCB24009, and Grant 20192BBE50063, and in part by the Science and Technology 5511 Project of Jiangxi Province, China, under Grant 20165BCB19010.

ABSTRACT A novel design method of microstrip diplexer without extra matching circuit is proposed in this paper. Because of the synthesizable circuit parameters and controllable transmission zeros (TZs) in composite resonator (CR) cell, diplexer A based on CR cell is proposed. By allocating TZs at center frequency of the opposite channel, as well as the using of impedance transformations of J-inverters, high isolation and good passband selectivity are realized in diplexer A without extra matching circuit. In order to improve the stopband performance, diplexer B based on coupled CR cells is proposed. Furthermore, diplexer B using the proposed design method is implemented by directly combining two bandpass filters (BPFs), which simplifies significantly the design process of diplexers. Diplexer A operated at 1/1.2 GHz and diplexer B operated at 1/1.5 GHz are designed and fabricated. The measured isolation characteristics in diplexer A and diplexer B are all higher than 40 dB. Good agreements between simulated and measured results are achieved, which successfully verifies the proposed design method of diplexers.

INDEX TERMS Composite resonator, extra matching circuit, high isolation, impedance transformation, microstrip diplexer, transmission zeros.

I. INTRODUCTION

Diplexers play an essential and significant role in the radio frequency (RF) front ends of the transceiver. Diplexers with multiple transmission zeros (TZs) and high isolation level are highly demanded in the modern wireless communication systems. Several advanced resonators such as slotline-loaded microstrip ring resonators [1], simple coupled line resonators [2], short stub-loaded composite right/left-handed resonators [3], defected ground resonators [4], [5], cavity resonators [6], [7], and coplanar waveguide resonators [8], [9] are successfully employed in bandpass filters (BPFs). The matching networks in diplexers ensure that BPFs match well in their working frequencies. Therefore, researches on the matching circuits have been also a hot point in recent years.

The associate editor coordinating the review of this article and approving it for publication was Feng Lin.

E-stub-loaded composite right-/left-handed (ESL-CRLH) resonators and quasi-lumped impedance matching network are applied to triplexer in [10]. Meanwhile, miniaturized size and high isolation are simultaneously acquired. In [11]–[13] T-shape resonator, spiral resonator, and composite right/left handed (CRLH) resonator are adopted as common resonators in diplexers for size reduction. Three-line coupled structure is utilized in the common port to achieve good isolation between two channels [14]. However, the process of obtaining the desired coupling in two channels may be a time-consuming work. T-junction as the most common and original approach is widely applied in the design of diplexers [15]–[21]. When the BPFs are designed at desired frequencies, BPFs are usually combined by a T-junction to keep good matching and isolation between two BPFs. Because the T-junction does not contribute the resonant mode and the microstrip lines related T-junction inevitably occupy extra area of the

circuit, T-junction can be seen as extra matching circuit in diplexers. By using I/O stub-loaded resonator [16], separated electric and magnetic coupling (SEMC) [17], embedded scheme resonator (ESR) [18], and signal-interference stepped-impedance lines [19], TZs are created at both sides of the passband, improving the selectivity of both channels.

In [8], a method of manipulating attenuation poles is proposed for diplexer design, and its isolation performance is improved greatly. However, lumped elements shall be used in the final circuit. Half-wavelength tapped-fed stepped-impedance resonators are proposed as matching circuits for microstrip triplexers in [22]. The stepped-impedance resonators serve as a through pass at the center frequency of a BPF. Diplexers with fully reconfigurable characteristics are proposed in [23] and [24], TZs are observed in the opposite channel, the matching conditions and processes between two channels are not studied in detail. In [25], the concept of dual-behavior resonator (DBR) is proposed. Then a different concept, called the composite resonator (CR), is proposed in [26] and the synthesis theory of BPFs is developed from lumped circuit. Both DBR and CR have the advantages of being independently controllable TZs and having synthesizable circuit parameters. Nevertheless, studies on the diplexer without extra circuit based on the synthesis theory of BPF using CR cells are still rare.

In this paper, diplexer A based on CR cells is synthesized by lumped element circuit and ideal transmission line circuit without extra matching network. Upon the proposed design method, diplexer B based on the coupled CR cells is proposed to improve the stopband performance. Compared with the diplexers using T-junction, the proposed diplexers can be directly combined by two BPFs without T-junction, which simplifies the design process. Diplexer A operated at 1/1.2 GHz and diplexer B operated at 1/1.5 GHz are designed and fabricated to verify the proposed design method can be used to design high isolated diplexers with different frequency ratios. The measured isolation level of the proposed two diplexers are higher than 40 dB. Moreover, simulated and measured results match well with each other.

The rest of this paper is arranged as follows. In Section II, BPFs using CR cells are analyzed and their applications to diplexers are discussed. Moreover, the synthesis and design method of the diplexer A without extra matching circuit are further put forward. In Section III, diplexer B based on coupled CR cells is designed by the aforementioned design method. Finally, the conclusions are presented in Section IV.

II. DIPLEXER A BASED ON CR CELLS

A. BPFS USING CR CELLS

Fig. 1(a) is the equivalent circuit of a second order BPF using shunted LC resonator cells and J-inverters. The correlation among inductance (L_{ri}), capacitance (C_{ri}) and J-inverters is constrained by [26]

$$L_{ri} = \frac{1}{\omega_0^2 C_{ri}} \ (i = 1, 2), \quad J_{01} = \sqrt{\frac{G_0 FBW \omega_0 C_{r1}}{\Omega_c g_0 g_1}} \tag{1}$$

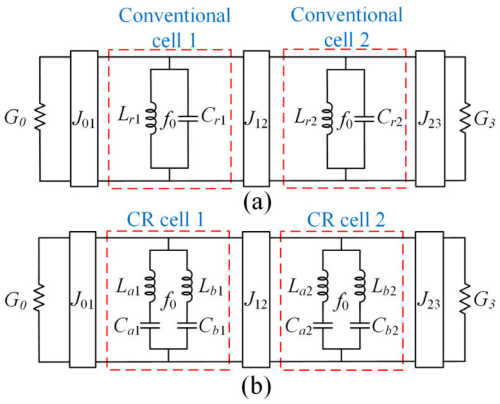

FIGURE 1. Equivalent circuit of second order BPFs. (a) Using Conventional shunted *LC* resonator cells and *J*-inverters. (b) Using CR cells and *J*-inverters.

$$J_{12} = \frac{FBW \omega_0}{\Omega_c} \sqrt{\frac{C_{r1} C_{r2}}{g_1 g_2}}, \quad J_{23} = \sqrt{\frac{G_3 FBW \omega_0 C_{r2}}{\Omega_c g_2 g_3}} \tag{2}$$

where ω_0 and FBW are the center angular frequency and the fractional bandwidth of the BPF, respectively. When the lowpass prototype filter is selected, element values g_0, g_1, g_2, and g_3 are determined. As to a BPF with center frequency of ω_0, its bandwidth can be changed by adjusting the values of J_{01} and C_{r1}. The lumped element values for second order Chebyshev lowpass prototype filter are given as $g_0 = 1$, $g_1 = 0.4489$, $g_2 = 0.4078$ and $g_3 = 1.1008$ [27]. G_0 and G_3 indicate conductance of 0.02 S.

The equivalent circuit of the second order BPF using CR cells and J-inverters is displayed in Fig. 1(b). Circuit parameters can be calculated by [26]

$$L_{ri} = \frac{2L'_{ai} L'_{bi}}{L'_{ai} + L'_{bi}} \quad (i = 1, \ 2) \tag{3}$$

$$L'_{ai} = \frac{\left(1 - \left(\frac{\omega_{ai}}{\omega_0}\right)^2\right)^2}{1 + \left(\frac{\omega_{ai}}{\omega_0}\right)^2} L_{ai},$$

$$L'_{bi} = \frac{\left(1 - \left(\frac{\omega_{bi}}{\omega_0}\right)^2\right)^2}{1 + \left(\frac{\omega_{bi}}{\omega_0}\right)^2} L_{bi} \tag{4}$$

where ω_{ai} and ω_{bi} are the angular frequencies of TZs that are generated by series $L_{ai}C_{ai}$ and $L_{bi}C_{bi}$ resonators, respectively.

Comparisons of the theoretical frequency responses between BPFs using conventional cells and CR cells are depicted in Fig. 2. Evidently, the same transmission characteristics in passband are obtained except that the BPF using CR cells owns four extra TZs, which greatly improves the selectivity of the filter. These TZs named TZ_1, TZ_2, TZ_3, and TZ_4 are generated by series $L_{a2}C_{a2}$, $L_{a1}C_{a1}$, $L_{b1}C_{b1}$, and $L_{b2}C_{b2}$ resonators, respectively. Moreover, TZ_2 and TZ_3 located near the passband are called the inner TZs, while TZ_1, and TZ_4 are called the outer TZs.

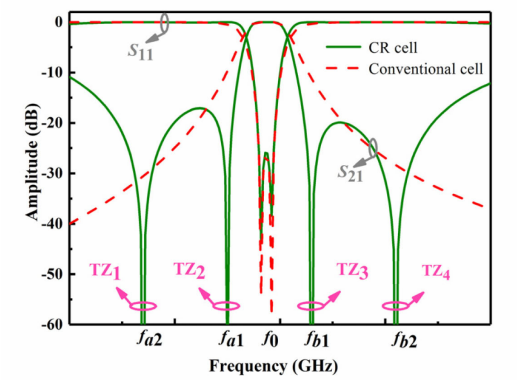

FIGURE 2. Theoretical frequency responses of the second order BPF by using conventional cells (dashed line) and CR cells (solid line).

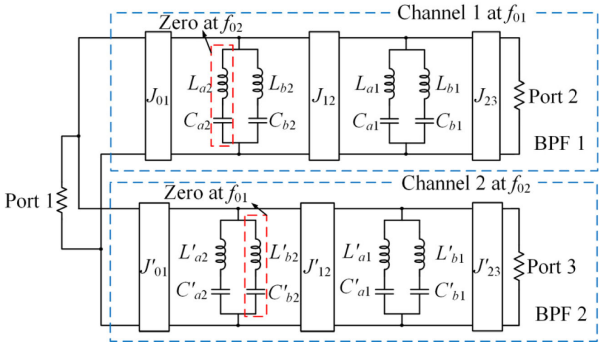

FIGURE 3. Structure of the proposed diplexer A using lumped element circuit.

TABLE 1. Element values in Fig. 3. (Unit: f: GHz, L: nH, C: pF).

BPF 1	f_{01}	J_{01}	J_{12}	J_{23}	L_{a1}	L_{a2}
	1.0	0.0221	0.0449	0.0387	5.00	5.00
	L_{b1}	L_{b2}	C_{a1}	C_{a2}	C_{b1}	C_{b2}
	4.52	4.09	6.25	7.92	4.63	4.30
BPF 2	f_{02}	J'_{01}	J'_{12}	J'_{23}	L'_{a1}	L'_{a2}
	1.2	0.0218	0.0485	0.0424	5.00	5.00
	L'_{b1}	L'_{b2}	C'_{a1}	C'_{a2}	C'_{b1}	C'_{b2}
	4.52	4.09	4.19	5.07	3.32	3.16

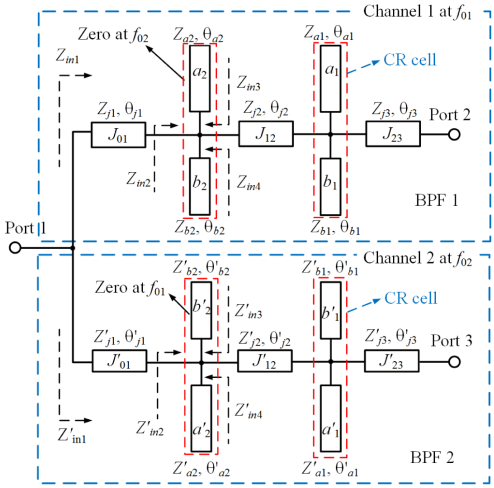

FIGURE 4. Structure of the proposed diplexer A using ideal transmission line circuit.

B. IMPLEMENTATION OF DIPLEXER A

According to the synthesis theory of CR cell based BPF mentioned above, diplexer A is proposed. Fig. 3 depicts the proposed diplexer A using lumped elements. The center frequency of the Channel 1 in the diplexer A is designed at 1 GHz (f_{01}). The center frequency of the Channel 2 is designed at 1.2 GHz (f_{02}). As can be observed, seriesLC resonators $L_{a2}C_{a2}$ and $L'_{b2}C'_{b2}$ resonate at f_{02} and f_{01}, respectively. The proposed diplexer A is directly combined by BPF 1 and BPF 2 without extra matching circuit. The frequency response of diplexer A using lumped element circuit is shown in Fig. 5 (solid line). As expected, four TZs are obtained in each channel. Besides, outer TZs at f_{02} and f_{01} are observed. The isolation is all higher than 35 dB from 0.8 GHz to 1.4 GHz. The lumped element values in Fig. 3 are listed in the Table 1.

In order to realize the diplexer A, it is necessary to transform lumped element circuit into ideal transmission line circuit, series LC resonators of CR cells in Fig. 3 are implemented by quarter-wavelength microstrip open stubs (a_i, b_i, a'_i, b'_i, $i = 1, 2$). The impedance of open stub is determined by

$$Z_{ai} = \frac{4}{\pi}\sqrt{\frac{L_{ai}}{C_{ai}}} \tag{5}$$

The electrical lengths of open stubs (θ_{ai}, θ_{bi} and θ'_{ai}, θ'_{bi}) are $\pi/2$ at the frequencies of TZs. J-inverters are realized by quarter-wavelength microstrip lines. The impedance of J-inverters is calculated by $Z_j = 1/J$ and the electrical lengths of J-inverters (θ_j and θ'_j) are $\pi/2$ at the center frequency of the BPF.

Therefore, the structure of the proposed diplexer A using ideal transmission line model is exhibited in Fig. 4. Z_{in} and Z'_{in} denote the input impedance of each branch. In addition, θ_{a2} and θ'_{b2} are set as $\pi/2$ at f_{02} and f_{01}, respectively.

Next, further exploration about the matching mechanism of Channel 1 and Channel 2 is carried out. Because the electrical lengths θ_{a2} and θ'_{a2} are $\pi/2$ at f_{02} and f_{01}, the input impedance Z_{in3} and Z'_{in3} of open stubs a_2 and b'_2 are calculated by

$$\begin{cases} Z_{in3} = -jZ_{a2}\cot\theta_{a2} = 0 & \text{at } f_{02} \\ Z'_{in3} = -jZ'_{b2}\cot\theta'_{b2} = 0 & \text{at } f_{01} \end{cases} \tag{6}$$

Then the input impedance of Z_{in2} and Z'_{in2} is decided by

$$\begin{cases} Z_{in2} = \dfrac{Z_{in3}Z_{in4}}{Z_{in3}+Z_{in4}} = 0 & \text{at } f_{02} \\ Z'_{in2} = \dfrac{Z'_{in3}Z'_{in4}}{Z'_{in3}+Z'_{in4}} = 0 & \text{at } f_{01} \end{cases} \tag{7}$$

TABLE 2. Parameters of ideal transmission line model in Fig. 4. (Unit: Z: Ω, θ at 1.1 GHz: deg).

BPF 1	Z_{j1}	θ_{j1}	Z_{j2}	θ_{j2}	Z_{j3}	θ_{j3}	Z_{a1}
	42.2	73.8	22.3	90	25.8	86.4	36.1
	θ_{a1}	Z_{a2}	θ_{a2}	Z_{b1}	θ_{b1}	Z_{b2}	θ_{b2}
	110	33.2	124	48.9	89.9	50.7	82.3
BPF 2	Z'_{j1}	θ'_{j1}	Z'_{j2}	θ'_{j2}	Z'_{j3}	θ'_{j3}	Z'_{a1}
	59.4	96.3	26.8	90	23.6	91.8	43.5
	θ'_{a1}	Z'_{a2}	θ'_{a2}	Z'_{b1}	θ'_{b1}	Z'_{b2}	θ'_{b2}
	89.9	40	99.2	47	76.1	67.6	70.8

After impedance transformation of the J-inverters (J_{01} and J'_{01}), the input impedance of Z_{in1} and Z'_{in1} in Fig. 4 must satisfy

$$\begin{cases} Z_{in1} = Z_j \dfrac{Z_{in2} + jZ_j \tan\theta_j}{Z_j + jZ_{in2} \tan\theta_j} = jZ_j \tan\theta_j & \text{at } f_{02} \\ Z'_{in1} = Z'_j \dfrac{Z'_{in2} + jZ'_j \tan\theta'_j}{Z'_j + jZ'_{in2} \tan\theta'_j} = jZ'_j \tan\theta'_j & \text{at } f_{01} \end{cases} \tag{8}$$

Furthermore, in order to meet the conditions of no reflection at one operation band and total reflection at the other operation band, the equations (9) must be satisfied

$$\begin{cases} Z_{in1} = \infty \;\&\; Z'_{in1} = 50\Omega & \text{at } f_{02} \\ Z'_{in1} = \infty \;\&\; Z_{in1} = 50\Omega & \text{at } f_{01} \end{cases} \tag{9}$$

In Fig. 4, equations (8) is equal to (9) under the circumstance of following equations

$$\begin{cases} \theta_j = \dfrac{n\pi}{2}, n = 1, 2, \cdots, N & \text{at } f_{02} \\ \theta'_j = \dfrac{n\pi}{2}, n = 1, 2, \cdots, N & \text{at } f_{01} \end{cases} \tag{10}$$

For the compactness of circuit, n = 1 is selected. Finally, equation (9) is met in Fig. 4.

The frequency response of diplexer A using ideal transmission line model is presented in Fig. 5 with dashed line. Apparently, the simulated results of ideal transmission line model agree well with calculated results of lumped elements model, which verifies the design method of the proposed diplexer. The parameters in Fig. 4 are listed in Table 2.

C. EXPERIMENT RESULTS OF DIPLEXER A

Fig. 6 shows the photograph of the fabricated diplexer and the geometrical dimensions are: $w_a = 0.6$, $l_b = 28.75$, $w_b = 0.75$, $l_c = 20.65$, $w_c = 2.65$, $l_d = 22.6$, $w_d = 2$, $l_e = 28.65$, $w_e = 1.25$, $l_f = 26.6$, $w_f = 0.95$, $l_g = 21.05$, $w_g = 0.6$, $l_h = 23.25$, $w_h = 0.5$, $l_i = 24.75$, $w_i = 0.6$, $l_j = 25$, $w_j = 1.8$, $l_k = 25.5$, $w_k = 1.5$, $l_m = 24.75$, $w_m = 0.7$, $l_n = 27.25$, $w_n = 0.45$, $l_o = 34.8$, $w_o = 1.95$, $l_p = 32.1$, and $w_p = 1.3$ (unit: mm). The overall size of diplexer is 60.24 mm × 49.82 mm about 0.52 λ_g × 0.43 λ_g, where the λ_g denotes the guided wavelength at the lower channel frequency. Simulated current distributions of the proposed diplexer are illustrated in Fig. 7. As depicted,

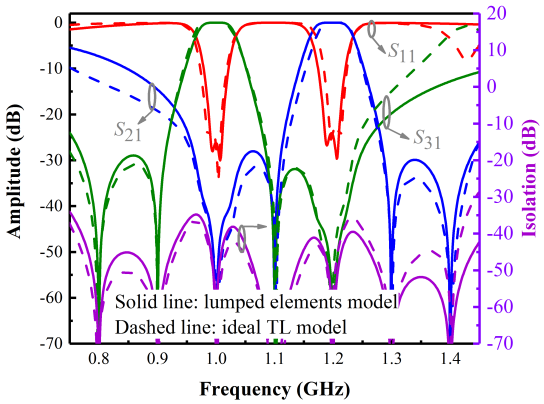

FIGURE 5. Frequency responses of the proposed diplexer A using lumped elements model (solid line) and ideal transmission line model (dashed line).

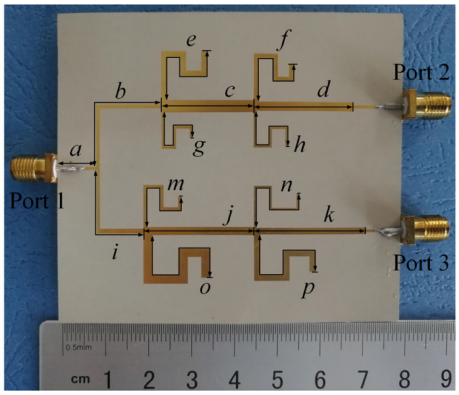

FIGURE 6. Photograph of the fabricated diplexer A.

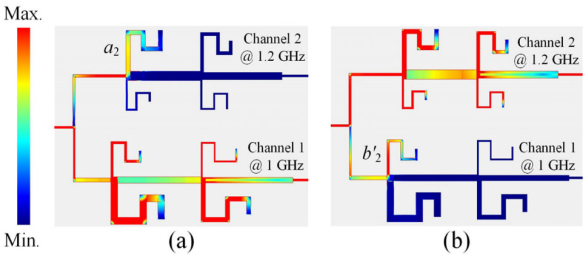

FIGURE 7. Simulated current distributions of the proposed diplexer A at (a) 1 GHz and (b) 1.2 GHz.

when diplexer A is working in Channel 2, open stub a_2 in Channel 1 resonates and no current passes Channel 1. Open stub b'_2 in Channel 2 resonates and there is no current passing Channel 2 when diplexer A is working in Channel 1.

The proposed diplexer A is simulated and fabricated on the RT6010LM substrate. The relative dielectric constant is 10.2 and thickness is 0.635 mm. The simulated and measured results are shown in Fig. 8. As observed in Fig. 8(a), the measured center frequencies of the two channels are 0.99 and 1.18 GHz with fractional bandwidth (FBW) of 5.8% and 6.4%, respectively. Frequency discrepancy between the

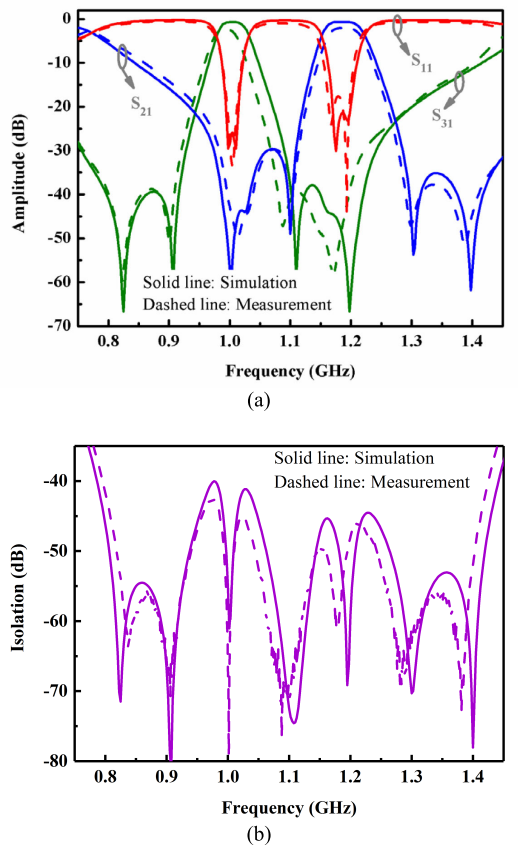

FIGURE 8. Simulated and measured results of the proposed diplexer A. (a) Insert loss and return loss. (b) Isolation.

simulated and measured results mainly originates from the fabrication tolerance. The measured minimum insertion loss is 2.09 dB for Channel 1, and 1.88 dB for Channel 2. The measured return loss for two channels is greater than 17.7 dB. Moreover, the measured isolation between two channels is higher than 43 dB from 0.8 GHz to 1.4 GHz in Fig. 8(b). The measured results show a good agreement with the simulated results. However, due to the direct connected structure, transmission characteristics of the diplexer A in the lower stopband are poor and need to be improved.

III. DIPLEXER B BASED ON COUPLED CR CELLS

A. DESIGN OF DIPLEXER B

In order to improve the poor lower and upper stopband performance in diplexer A, one effective way is to replace the quarter-wavelength microstrip lines of J_{12} and J'_{12} by gap coupling.

The structure of the diplexer B based on coupled CR cells and parameter values of circuit are shown in Fig. 9. It should be noted that the coupled CR cell in each channel is identical. Therefore, the distribution of TZs will be different from diplexer A. Uniform impedance open stubs in Fig. 4 are substituted by stepped-impedance open stubs for size reduction and stopband extension [28]. The equivalent electrical length of stepped-impedance open stub is calculated by

$$\theta_{T1} = \theta_3 + \arctan\left(\frac{R}{\tan\theta_3}\right) \tag{11}$$

where R is the impedance ratio of Z_3/Z_4.

In Fig. 9, a and a' denotes the stepped-impedance open stubs. Similarly, the equivalent electrical lengths of a and a' are set as $\pi/2$ at f_{02} and f_{01}, respectively. Thereby, the following equations are satisfied naturally in Fig. 9.

$$\begin{cases} Z_{in3} = -jZ_{T1}\cot\theta_{T1} = 0 & \text{at } f_{02} \\ Z'_{in3} = -jZ'_{T1}\cot\theta'_{T1} = 0 & \text{at } f_{01} \end{cases} \tag{12}$$

The same equations (7) and (8) as elaborated in Section II for matching conditions are used to design the proposed diplexer B. Finally, we get the following equations:

$$\begin{cases} Z_{in1} = \infty & \text{at } f_{02} \\ Z'_{in1} = \infty & \text{at } f_{01} \end{cases} \tag{13}$$

Therefore, excellent matching level is attained in Fig. 9 without extra matching circuit. Frequency responses of diplexer B are plotted in Fig. 10. The center frequencies of Channel 1 and Channel 2 are 1 GHz and 1.5 GHz. Good isolation and multiple TZs are simultaneously obtained except that a spurious frequency is observed at f_s about 0.4 GHz in Fig. 10. It is caused by the resonance of the part which connects to port 1.

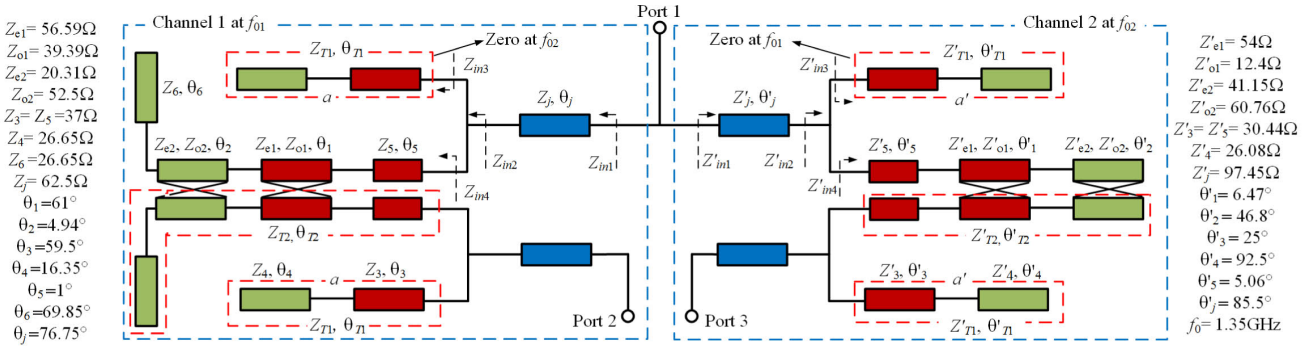

FIGURE 9. Structure and parametric values of diplexer B based on coupled CR cells.

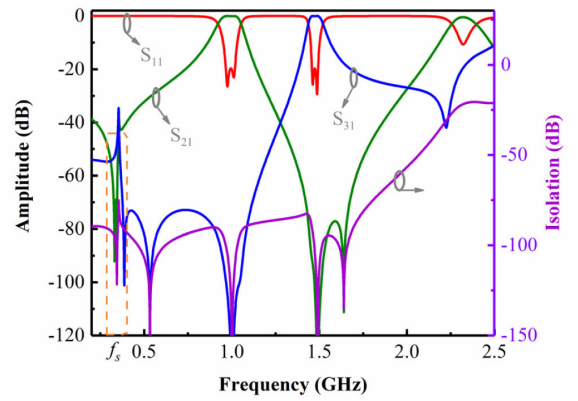

FIGURE 10. Frequency response of the proposed diplexer B in Fig. 9.

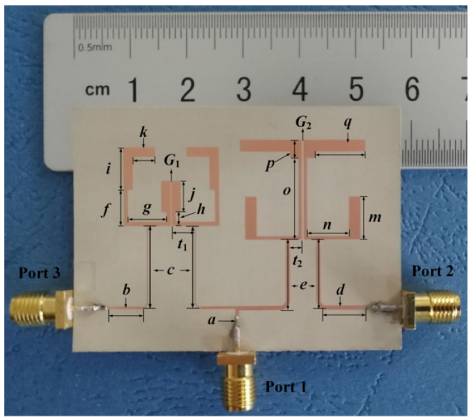

FIGURE 11. Photograph of the fabricated diplexer B.

The design guidelines of the proposed diplexers are summarized into the following steps:

1) According to the given center frequencies of Channel 1 and Channel 2 (i.e., f_{01}, and f_{02}), synthesize the open stub to generate TZ at center frequency of the opposite channel.
2) Set the electrical length of J-inverters $\theta_j = \pi/2$ at f_{02} and $\theta_j' = \pi/2$ at f_{01}, respectively.
3) According to the filter specifications such as FBW and passband ripple, design the rest part of the BPF.
4) Combine two designed BPFs directly and the diplexer can be achieved.

B. EXPERIMENT RESULTS OF DIPLEXER B

The photograph of diplexer B is displayed in Fig. 11, and its geometrical dimensions are $w_a = 0.6$, $l_b = 6.05$, $w_b = 0.4$, $l_c = 14.7$, $w_c = 0.2$, $l_d = 7.3$, $w_d = 0.7$, $l_e = 12.5$, $w_e = 0.7$, $l_f = 6.4$, $w_f = 0.7$, $l_g = 6.9$, $w_g = 0.7$, $l_h = 2.45$, $w_h = 0.7$, $l_i = 7.45$, $w_i = 1.6$, $l_j = 5.5$, $w_j = 1.6$, $l_k = 4$, $w_k = 1.6$, $l_m = 7.65$, $w_m = 2$, $l_n = 7.5$, $w_n = 0.55$, $l_o = 14.5$, $w_o = 0.55$, $l_p = 3.15$, $w_p = 2$, $l_q = 8.85$, $w_q = 2$, $G_1 = 0.2$, $G_2 = 0.4$, $t_1 = 4$, and $t_2 = 2.15$ (unit: mm). The design of different widths (w_b and w_c) in

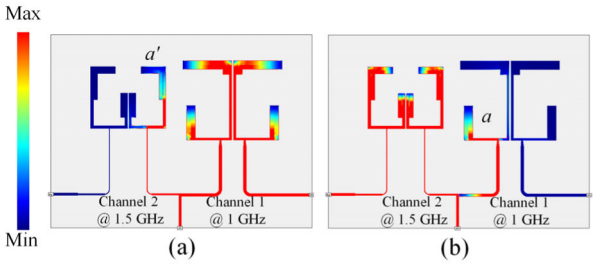

FIGURE 12. Simulated current distributions of the proposed diplexer B at (a) 1 GHz and (b) 1.5 GHz.

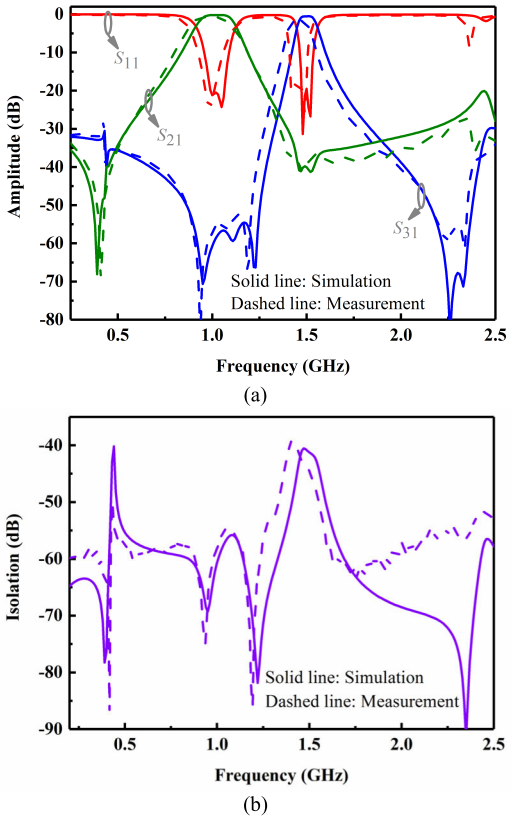

FIGURE 13. Simulated, and measured results of the diplexer B. (a) Frequency response. (b) Isolation response.

J-inverter is to suppress the spurious resonance about 0.43 GHz in Fig. 13(a). The overall size excluding the feed lines of diplexer B is 45.8 mm × 29.45 mm, about 0.39 λ_g × 0.25 λ_g, where the λ_g is the guided wavelength at the lower channel frequency.

The proposed diplexer B is also simulated and fabricated on the RT6010LM substrate. The relative dielectric constant and thickness of the substrate are 10.2 and 0.635 mm, respectively. The diplexers are measured by using the Agilent E5071C vector network analyzer.

Furthermore, analysis of the current distribution at the working bands in diplexer B is conducted. When diplexer B is working at 1 GHz (Channel 1) in Fig. 12(a), there are no current passing through 1.5 GHz (Channel 2), but the stub a' in Channel 2 resonates. Moreover, the stub a in Channel 1

TABLE 3. Comparisons between references and proposed diplexers.

Ref. No	Freq. (GHz)	Freq. Ratio	Size ($\lambda_g \times \lambda_g$)	Iso. (dB)	TZs
[5]	1.80/2.45	1.36	0.14×0.31	>30	4
[11]	1.95/2.14	1.10	0.36×0.38	>35	7
[14]	1.00/1.20	1.20	0.55×0.40	>37	0
[17]	1.80/2.45	1.36	0.69×0.27	>38	6
[18]	1.96/2.13	1.09	0.23×0.23	>25	4
[20]	9.50/10.5	1.11	3.19×1.02	>35	5
[21]	1.79/2.05	1.15	N/A	>34	0
diplexer A	**0.99/1.18**	**1.19**	**0.52×0.43**	**>43**	**8**
diplexer B	**0.99/1.46**	**1.47**	**0.39×0.25**	**>40**	**7**

Ref. No: Reference number, Freq. Ratio: Frequency ratio, Iso.: Isolation.

resonates and no current passes through Channel 1 when diplexer B is working at Channel 2 in Fig. 12(b).

The simulated and measured results of diplexer B are illustrated in Fig. 13. In Fig. 13(a), the measured center frequencies are 0.99 GHz and 1.46 GHz with the FBW of 21.3% and 7.9%. Such a frequency shift might be attributed to the fabricated error and deviation of the thickness of dielectric. The measured minimum insertion loss is 1.15 dB and 1.5 dB in the Channel 1 and Channel 2, respectively. The measured maximum return loss in the both channels are higher than 18 dB. As expected, compared with diplexer A, the lowpass property has been eliminated in diplexer B. Moreover, the lower and upper stopband rejections are improved. Multiple TZs are observed, which improves the isolation characteristics and the stopband performance. Furthermore, the isolation level is higher than 40 dB from 0.2 GHz to 2.5 GHz in Fig. 13(b). Finally, the comparisons of proposed diplexers with other diplexers in references are listed in the Table 3. It is found that the proposed diplexers A and B show the advantages of multiple TZs and higher isolation.

IV. CONCLUSION

In this paper, a novel design method for high isolation diplexers is proposed. Due to the distribution of TZs at center frequency of the opposite channel and the using of impedance transformations of J-inverters, diplexers can be directly combined by two BPFs. Therefore, the proposed diplexers are accomplished without extra matching circuit, which greatly simplifies the design process of diplexers. Upon this method, diplexer A using CR cells and diplexer B using coupled CR cells with different frequency ratio are simulated and fabricated. Multiple TZs and high isolation are realized in the simulated and measured results. Moreover, simulated results have a great agreement with measured results, which demonstrates the proposed design method of diplexer.

REFERENCES

[1] D. Chen, L. Zhu, H. Bu, and C. Cheng, "A novel planar diplexer using slotline-loaded microstrip ring resonator," *IEEE Microw. Wireless Compon. Lett.*, vol. 25, no. 11, pp. 706–708, Nov. 2015.

[2] K.-D. Xu, D. Li, and Y. Liu, "High-selectivity wideband bandpass filter using simple coupled lines with multiple transmission poles and zeros," *IEEE Microw. Wireless Compon. Lett.*, vol. 29, no. 2, pp. 107–109, Feb. 2019.

[3] M. Li, K.-D. Xu, J. Ai, and Y. Liu, "Compact diplexer using short stub-loaded composite right/left-handed resonators," *Microw. Opt. Technol. Lett.*, vol. 59, no. 6, pp. 1470–1474, Jun. 2017.

[4] H. Liu, W. Xu, Z. Zhang, and X. Guan, "Compact diplexer using slotline stepped impedance resonator," *IEEE Microw. Wireless Compon. Lett.*, vol. 23, no. 2, pp. 75–77, Feb. 2013.

[5] K. Song, Y. Zhou, Y. Chen, S. R. Patience, S. Guo, and Y. Fan, "Compact high-isolation multiplexer with wide stopband using spiral defected ground resonator," *IEEE Access*, vol. 7, pp. 31702–31710, 2019.

[6] X. Shang, Y. Wang, W. Xia, and M. J. Lancaster, "Novel multiplexer topologies based on all-resonator structures," *IEEE Trans. Microw. Theory Techn.*, vol. 61, no. 11, pp. 3838–3845, Nov. 2013.

[7] S.-W. Wong, Z.-C. Zhang, S.-F. Feng, F.-C. Chen, L. Zhu, and Q.-X. Chu, "Triple-mode dielectric resonator diplexer for base-station applications," *IEEE Trans. Microw. Theory Techn.*, vol. 63, no. 12, pp. 3947–3953, Dec. 2015.

[8] T. Ohno, K. Wada, and O. Hashimoto, "Design methodologies of planar duplexers and triplexers by manipulating attenuation poles," *IEEE Trans. Microw. Theory Techn.*, vol. 53, no. 6, pp. 2088–2095, Jun. 2005.

[9] T. Zheng, B. Wei, B. Cao, X. Guo, X. Zhang, L. Jiang, Z. Xu, and Y. Heng, "Compact superconducting diplexer design with conductor-backed coplanar waveguide structures," *IEEE Trans. Appl. Supercond.*, vol. 25, no. 2, Apr. 2015, Art. no. 1501304.

[10] K. Da Xu, M. Li, Y. Liu, Y. Yang, and Q. H. Liu, "Design of triplexer using E-stub-loaded composite right-/left-handed resonators and quasi-lumped impedance matching network," *IEEE Access*, vol. 6, pp. 18814–18821, 2018.

[11] X. Guan, F. Yang, H. Liu, and L. Zhu, "Compact and high-isolation diplexer using dual-mode stub-loaded resonators," *IEEE Microw. Wireless Compon. Lett.*, vol. 24, no. 6, pp. 385–387, Jun. 2014.

[12] X. Guan, F. Yang, H. Liu, Z. Ma, B. Ren, W. Huang, and P. Wen, "Compact, low insertion-loss, and wide stopband HTS diplexer using novel coupling diagram and dissimilar spiral resonators," *IEEE Trans. Microw. Theory Techn.*, vol. 64, no. 8, pp. 2581–2589, Aug. 2016.

[13] T. Yang, P.-L. Chi, and T. Itoh, "Compact quarter-wave resonator and its applications to miniaturized diplexer and triplexer," *IEEE Trans. Microw. Theory Techn.*, vol. 59, no. 2, pp. 260–269, Feb. 2011.

[14] F.-C. Chen, H.-T. Hu, R.-S. Li, J.-F. Chen, D. Luo, Q.-X. Chu, and M. J. Lancaster, "Design of wide-stopband bandpass filter and diplexer using uniform impedance resonators," *IEEE Trans. Microw. Theory Techn.*, vol. 64, no. 12, pp. 4192–4203, Dec. 2016.

[15] T. Yang, P.-L. Chi, and T. Itoh, "High isolation and compact diplexer using the hybrid resonators," *IEEE Microw. Wireless Compon. Lett.*, vol. 20, no. 10, pp. 551–553, Oct. 2010.

[16] C. F. Chen, C. Y. Lin, B. H. Tseng, and S. F. Chang, "High-isolation and high-rejection microstrip diplexer with independently controllable transmission zeros," *IEEE Microw. Wireless Compon. Lett.*, vol. 24, no. 12, pp. 851–853, Dec. 2014.

[17] J.-K. Xiao, Y. Li, and J.-G. Ma, "Compact and high isolated triangular split-ring diplexer," *Electron. Lett.*, vol. 54, no. 10, pp. 661–663, May 2018.

[18] B.-F. Zong, G.-M. Wang, Y.-W. Wang, and F. Wu, "Design of compact BPF and planar diplexer for UMTS using embedded-scheme resonator," *Radioengineering*, vol. 22, no. 4, pp. 1218–1223, Dec. 2013.

[19] R. Gómez-García, J.-M. Muñoz-Ferreras, and M. Sánchez-Renedo, "Signal-interference stepped-impedance-line microstrip filters and application to duplexers," *IEEE Microw. Wireless Compon. Lett.*, vol. 21, no. 8, pp. 421–423, Aug. 2011.

[20] S. Sirci, J. D. Martinez, J. Vague, and V. E. Boria, "Substrate integrated waveguide diplexer based on circular triplet combline filters," *IEEE Microw. Wireless Compon. Lett.*, vol. 25, no. 7, pp. 430–432, Jul. 2015.

[21] Z. Qi, X. Li, and J. Zeng, "Wideband diplexer design and optimization based on back-to-back structured common port," *IEEE Microw. Wireless Compon. Lett.*, vol. 28, no. 4, pp. 320–322, Apr. 2018.

[22] P.-H. Deng, M.-I. Lai, S.-K. Jeng, and C. H. Chen, "Design of matching circuits for microstrip triplexers based on stepped-impedance resonators," *IEEE Trans. Microw. Theory Techn.*, vol. 54, no. 12, pp. 4185–4192, Dec. 2006.
[23] D. Psychogiou, R. Gómez-García, and D. Peroulis, "Tune-all RF planar duplexers with intrinsically switched channels," *IEEE Microw. Wireless Compon. Lett.*, vol. 27, no. 4, pp. 350–352, Apr. 2017.
[24] D. J. Simpson, R. Gómez-García, and D. Psychogiou, "Single-/multi-band bandpass filters and duplexers with fully reconfigurable transfer-function characteristics," *IEEE Trans. Microw. Theory Techn.*, vol. 67, no. 5, pp. 1854–1869, May 2019.
[25] C. Quendo, E. Rius, and C. Person, "Narrow bandpass filters using dual-behavior resonators," *IEEE Trans. Microw. Theory Techn.*, vol. 51, no. 3, pp. 734–743, Mar. 2003.
[26] Z. Ma and Y. Kobayashi, "Design and realization of bandpass filters using composite resonators to obtain transmission zeros," in *Proc. 35th Eur. Microw. Conf.*, Oct. 2005, pp. 1255–1258.
[27] J. S. Hong and M. J. Lancaster, *Microwave Filter for RF/Microwave Application*. New York, NY, USA: Wiley, 2001.
[28] J.-T. Kuo and E. Shih, "Microstrip stepped impedance resonator bandpass filter with an extended optimal rejection bandwidth," *IEEE Trans. Microw. Theory Techn.*, vol. 51, no. 5, pp. 1554–1559, May 2003.

XUEHUI GUAN (M'11) received the B.S. degree in communication engineering from Jiangxi Normal University, Nanchang, China, in 1998, and the Ph.D. degree in electromagnetic fields and microwave techniques from Shanghai University, Shanghai, China, in 2007.

From 2007 to 2016, he was with East China Jiaotong University, Nanchang, as a Lecturer and an Associate Professor. In 2012, he was a Senior Researcher Associate with the School of Electrical and Electronic Engineering, City University of Hong Kong, Hong Kong. Since June 2013, he has been a Visiting Scholar with the School of Electrical and Electronic Engineering, Nanyang Technological University, Singapore. In 2016, he became a Professor with East China Jiaotong University. His current research interests include microwave passive circuits, high-temperature superconducting circuits, synthesis theory and realization of microwave filters, and antennas for wireless communications.

WANG LIU received the B.S. degree in electronic information engineering from Changsha University, Changsha, China, in 2017. He is currently pursuing the M.S. degree in communication and information system with East China Jiaotong University, China.

His current research interests include microstrip diplexers and planar filtering antenna for wireless communications.

BAOPING REN (S'16) received the B.S. degree in communication engineering and the M.S. degree in communication and information system from East China Jiaotong University, Nanchang, China, in 2011 and 2014, respectively, and the Ph.D. degree in microwave engineering from Saitama University, Saitama, Japan, in 2019.

From July 2014 to March 2019, he was a Research Associate with the Jiangxi RF Communications and Sensor Networks Key Laboratory, East China Jiaotong University, where he is currently an Assistant Professor. His current research interests include microwave circuits and devices, and high-temperature superconducting filters.

HAIWEN LIU (M'04–SM'13) received the B.S. degree in electronic system and the M.S. degree in radio physics from Wuhan University, Wuhan, China, in 1997 and 2000, respectively, and the Ph.D. degree in microwave engineering from Shanghai Jiao Tong University, Shanghai, China, in 2004.

From 2004 to 2006, he was a Research Assistant Professor with Waseda University, Kitakyushu, Japan. From 2006 to 2007, he was a Research Fellow with Kiel University, Kiel, Germany, where he was granted the Alexandervon Humboldt Research Fellowship. From 2007 to 2008, he was a Professor with the Institute of Optics and Electronics, Chengdu, China, where he was supported by the 100 Talents Program of Chinese Academy of Sciences. From 2009 to 2017, he was a Chair Professor with East China Jiaotong University, Nanchang, China. In 2014, he joined Duke University, Durham, NC, USA, as a Visiting Scholar. In 2015, he joined The University of Tokyo, Tokyo, as a Visiting Professor, where he was supported by the JSPS Invitation Fellowship. In 2016, he joined the City University of Hong Kong, Hong Kong, as a Visiting Professor. Since 2017, he has been a full-time Professor with Xi'an Jiaotong University, Xi'an, China. He has authored or coauthored more than 100 articles in international and domestic journals and conferences. His current research interests include electromagnetic modeling of high-temperature superconducting circuits, RF and microwave passive circuits and systems, synthesis theory and practices of microwave filters and devices, antennas for wireless terminals, and radar systems. He was a recipient of the National Talent Plan, China, in 2017. He was a Co-Chairman of the National Compressive Sensing Workshop of China, in 2011, an Executive Chairman of the National Antenna Conference of China, in 2015, and a Co-Chairman of the Communication Development Workshop of China, in 2016. He has served as the Editor-in-Chief for the *International Journal of RF and Microwave Computer-Aided Engineering* (Wiley), an Associate Editor for IEEE Access, and the Guest Chief Editor for the *International Journal of Antennas and Propagation*.

PIN WEN (S'16) received the B.S. degree in communication engineering and the M.S. degree in communication and information system from East China Jiaotong University, Nanchang, China, in 2012 and 2015, respectively. He is currently pursuing the Ph.D. degree in microwave engineering with Xi'an Jiaotong University, China.

In 2015, he became a Research Assistant with East China Jiaotong University. His current research interests include antenna theory, and design and superconducting filter design.